DINAME 2017 - Proceedings of the XVII International Symposium on Dynamic Problems of Mechanics
A. T. Fleury, D. A. Rade, P. R. G. Kurka (Editors), ABCM, São Sebastião, SP, Brazil, March 5-10, 2017

Hardware-in-the-loop optimization of an interaction controller for improved coupled dynamics

Gustavo J. G. Lahr[1], **Henrique B. Garcia**[1], **Thiago H. S. Silva**[1], **Glauco A. P. Caurin**[1]

[1] Robotics Manipulation Laboratory, Engineering School of Sao Carlos, University of Sao Paulo, Sao Carlos-SP, Brazil, {gjgl.lahr,henriqueborgesgarcia,thiagohsegreto} @gmail.com, gcaurin@sc.usp.br

Abstract: This paper presents the implementation of an optimization method to find, without previous knowledge of the environment characteristics, the best interaction controller parameters in order to revamp the coupled dynamics. The objective of this achievement is to improve various industrial robot applications that involves mechanical contact. An enhanced contact is accomplished by lowering the following metrics: rise time, total variation and steady state error. Hence, the impedance controller was one of the interaction control techniques chosen to be optimized, since it is one of the most successful in its field. In the experiments, a contact is established between a Kuka KR16 robot TCP and an aluminum platform, where the force data was acquired by a 6 axis force-torque sensor located in the robot's end-effector. Using a hardware-in-the-loop optimization approach, the force feed-back is processed by the NSGA-II algorithm and new individuals are developed. Each individual of the GA represents specific impedance controller parameters and as the generations passes, these values get more suitable for diminishing the mentioned metrics. Also, the relationship between damping and rise time, rise time and total variation versus the controller' stiffness, and the forces over time are further discussed.

***Keywords:* Industrial robots, interaction controller, mechanical contact, impedance control, multi-objective optimization**

INTRODUCTION

Mechanical contact is a weighting factor when it comes to a wide variety of robotic applications. Performing delicate surgeries (Jayender et al. 2006), manufacturing in shared environments with humans (Fryman and Matthias 2012) and stabilizing bionic orthesis (Caurin et al. 2011) are some examples of contact involved in robot processes. To achieve a suitable contact behavior, an estimation of the forces and torques acting on robot's TCP is required. However, knowing the net forces isn't enough, in order to really ensure stability and performance, an interaction controller must be implemented.

There are two main categories of interaction controllers: passive and active. The passive version does not require force and torque sensors feedback, but it requires the contacting environment to be structured and well known. Additionally, for good performance results, the robot should execute strictly predefined motions and should not change them during task execution. A robot with passive interaction controller can perform tasks faster when compared with the ones using the active controllers. However, it lacks versatility for industrial applications inasmuch as for every task a new end-effector must be designed and mounted. Active interaction controllers, on the other hand, allows the robot to re-adapt itself to unforeseen situations and unknown environments by recalculating its trajectory with the support of force-torque sensors feedback (Siciliano and Villani 1999).

One example of successful active interaction controllers is the impedance control (Hogan 1985). It provides stability on free motion if the controller itself is stable (Hogan 1987), however, although this property is guaranteed, excess of oscillations may happen during contact. This effect, characterized by intermittent interaction, is due to the transition from unconstrained to constrained motion and it's called chatter or bounce (Love and Book 1995). In this case, the desired scenario, where the bounce effect is minimized, is established using a coupled dynamic in which the rise time and overshoot are the smallest. These two metrics are directly related to the amount of bouncing, and are intrinsically related to the impedance controller and to the environment characteristics.

A possibility to enhance the performance during interaction is to estimate the environment parameters. An usual model for interaction in the literature is shown at Fig. 1a. The robot-controller is modeled as a second order system, and the environment as a first-order (Erickson et al. 2003). The resulting dynamics is also modeled, so during interaction, the force measured at the sensor is obtained for the coupled system. Different methods for estimation are possible: Erickson et al. (2003) compared four different methods, either on-line and off-line; Coutinho and Cortesao (2009) implemented a multiple observers method and another method which does not need the position values of robot's TCP (Coutinho and Cortesao 2012). Robot and environment, however, contain uncertainties. Lahr et al. (2016) experimented a stiff contact task and it proved to be different from the second order model proposed, in a relatively controlled situation, being that Erickson et al.(2003) also compared the methods using a well known environment. The manipulator is also often a source

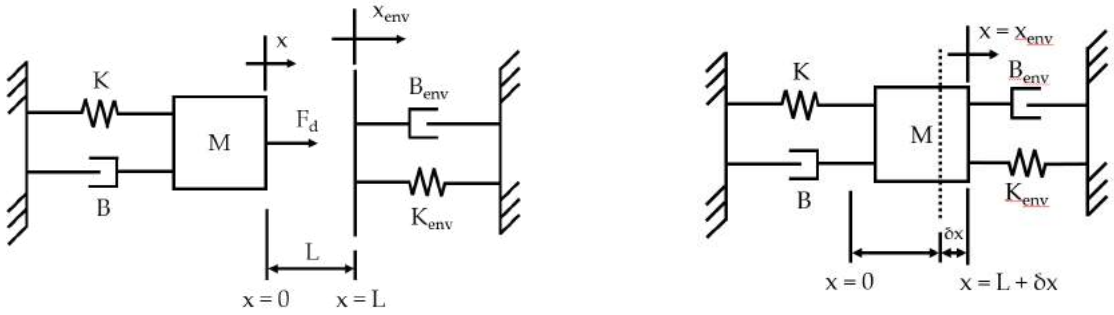

Figure 1: Modeling for interaction situation along 1 DoF: (a) before contact; (b) during contact

of not modeled dynamics, which could be neglected depending on the application (Lange et al. 2013), but for many a situation it should be taken into account.

We propose a method which does not need to estimate the environment's parameters, neither needs to take into account the nonlinearities. With the implementation of a hardware-in-the-loop optimization, where the metrics are obtained from real experiments within the optimization loop, it is possible to optimize the impedance controller parameters without considering non-modeled dynamics on robot-tool-environment. This is possible due the use of a genetic algorithm (NSGA-II) for a simplified one degree of freedom contact task. Experimental results are presented and discussed.

Impedance controller

In order to simplify the modeling, it is possible to approach the problem along one degree of freedom (DoF), where the robot may receive three parameters: mass, M, spring, K, and damper, B. If the robot is required to follow a desired position $x_0(t)$, with derivatives $\dot{x}_0(t)$ and $\ddot{x}_0(t)$, there is the actual position, $x(t)$, which may present a difference between unconstrained and constrained motion. Figure 1a shows the robot modeled as a second order system, and the environment as a first order with K_{env} and B_{env} parameters. When contact is achieved (figure 1b) the coupled system robot+environment now displays a displacement between resting position and actual position, denoted by $\delta x(t)$, which is equivalent to $\delta x(t) = x(t) - L$, where L is the distance between robot's initial position and the environment. Equation (1) model this situation for a desired contact force, F_d, and the actual interaction force, F_{int}. Applying Laplace transform on (1) with initial conditions null, it is possible to obtain (2)

$$M[\ddot{x}(t) - \ddot{x}_0(t)] + B[\dot{x}(t) - \dot{x}_0(t)] + K[x(t) - x_0(t)] = F_d(t) - F_{int}(t) \Rightarrow \tag{1}$$

$$\Rightarrow (Ms^2 + Bs + K)(X(s) - X_0(s)) = F_d(s) - F_{int}(s) \Rightarrow (Ms^2 + Bs + K)\Delta X(s) = \Delta F(s) \tag{2}$$

Proposed by Hogan (1985), the impedance controller has gained ground in research and development processes. Its wide applicability is given by the fact that it implements a controller relating the mechanical quantities flow and effort, velocities and forces on the linear case - respectively. This kind of implementation is called indirect force control (Villani and de Schutter 2008), since it does not deal with a pure force controller, instead, parameters deal with the relationship between force and position. This means that an impedance is basically a mapping from the wrenches space (F - generalized forces) to the twists space (M - general movements): $F^6 \rightarrow M^6$. The ratio shown by (3) explicitly shows how the system's impedance ($Z(s)$) correlates efforts ($F(s)$) and flows ($X(s)$). The concept applied to the impedance controller is the same to stiffness and compliance controllers (Salisbury 1980, Mason 1981), relating flow and efforts. However, these last two methods are better implemented for quasi static or static situations (Villani and de Schutter 2008), do not taking into account variables with higher order in time.

$$\frac{\Delta F(s)}{\Delta X(s)} = Z(s), \; where \; Z(s) = Ms + B + \frac{K}{s} \tag{3}$$

Although Hogan (1985) makes the case that an impedance does not have to be linear, it is a common implementation a controller which is a second order and linear time invariant (LTI) (Buerger and Hogan 2007), denoted by (3), and implemented in this work for a one degree of freedom. Its implementation on discrete systems, as industrial robots, may be found at Lahr et al. (2016), using discretization implementation.

Related work

Optimization methods for impedance controllers have already been subjects of study in related works. Particle Swarm Optimization (PSO) algorithm was used as impedance controller parameters tuner by Medhi and Boubaker (2011), in a

simulated model of a planar 3 DOF manipulator. Yet, the transition between unconstrained to constrained motion isn't modeled, letting the nonlinearities of the contact overlooked. Erchao (2016) gauges the controller parameters considering a multi-objective optimization in which the objective functions are: overshoot, settling time, and steady-state error. Using only force data feedback, the technique embodies a Pareto optimality along one DoF, still in constrained movement only. This work, on the other hand, embraces the nonlinearity of the unconstrained/constrained motion transition as well as the position feedback.

EXPERIMENTS

Multi-objective optimization

Many classical optimization methods use gradients, which requires knowledge of the objective function in question. Often this is not known or has nonlinearities that makes a computationally expensive method. Some modern approaches deal with the use only of values of this function without knowing its derivatives (Rao 2009), such as genetic algorithms (GA). Using the concept of population, which is composed of several individuals, the GA seeks to generate compositions of the objective function values for each individual within the space of possible solutions. This allows to attenuate the local minima problem, given the variability in the results obtained. This work implemented the NSGA-II algorithm (Deb et al. 2002), which is capable to deal with multi-objective problems and multiple variables. The input vector for the metrics evaluation is the force vector in the Z axis, denoted by F_z.

NSGA-II being multi-objective means that the optimization can be conducted based on more than one criterion desirable to obtain the best population through evolution. It is an important feature in the case of the implementation of this work, once a good contact state has low rise time and low overshoot+settling time. These metrics, however, are trade offs between themselves: lower the rise time, higher the overshoot and settling time. This motivates the search for the best values through the metrics.

As settling time and overshoot are quantities that have different numerical values, the use of weights for balancing both during optimization would be necessary. The process may be facilitated by using a quantity which relates both of them, called total variation (TV). This is obtained by the sum of all the differences between consecutive peaks and valleys of the objective function, F_z, according to equation (4) (Boyd and Barratt 1991). Being i related to the vector index which the evaluation algorithm is analyzing, N is the size of the force vector recorded.

$$TV(f) = \sup_{0 \leq t_1 \leq \ldots \leq t_N} \sum_{i=1}^{N-1} |F_z(t_i) - F_z(t_{i+1})| \tag{4}$$

For the rise time rule, which is the metric that measures the time taken for the system to reach its final value for the first time, we used the value from 0% and 100% (equation (6)) (Ogata 2010). The final value, $\bar{f}_{end}$, is obtained by the mean of the 50 final values of the force vector, F_z, with N number of points, as described by equation (5).

$$\bar{f}_{end} = \frac{\sum_{i=N-50}^{N} F_{z_i}}{50} \tag{5}$$

$$T_r = t_r, \text{ where } \bar{f}_{end} - F_z(t_r) < 0 \text{ for the first time} \tag{6}$$

Also, since the impedance controller does not take into account an integrative portion by itself, i.e., there is a steady state error associated. This metric was also inserted as another objective, denoted by E_ss and described by equation (7), obtained by the subtraction of the reference force value, F_{d_z}, and the final force vector value, $F_{z_{end}}$.

$$E_{ss} = \left| F_{d_z} - F_{z_{end}} \right| \tag{7}$$

So the problem is characterized by three variables ($\mathbf{X} = [M, B, K]^T$) with three goals defined as $f_1(\mathbf{X}) = TV$, $f_2(\mathbf{X}) = T_r$ and $f_3(\mathbf{X}) = E_{ss}$, and the optimization problem is presented in equation (8). The constraints are defined as each variable boundary as $10\ kg \leq M \leq 60\ kg$, $100\ Ns/m \leq B \leq 1000\ Ns/m$ e $100\ N/m \leq K \leq 4000\ N/m$ and, from empirical experimentation, constraint for the damping value, $\zeta = \frac{B}{2\sqrt{MK}}$.

$$\begin{aligned} \min_{\mathbf{X}} \quad & (f_1(\mathbf{X}), f_2(\mathbf{X}), f_3(\mathbf{X})) \\ & \mathbf{X} = [M, B, K]^T \\ \text{s.t.} \quad & 10\ kg \leq M \leq 20\ kg \\ & 100\ Ns/m \leq B \leq 1000\ Ns/m \\ & 1000\ N/m \leq K \leq 4000\ N/m \\ & 0.5 \leq \zeta \leq 0.95 \end{aligned} \tag{8}$$

Experimental implementation

To achieve the desired behavior for the study, a contact is settled between a tool mounted at the extremity of a Kuka KR16 Robot and an aluminum profile structure. The robot movement is constrained in only one DoF, being the one which is the robot Z world's coordinate frame, perpendicular to the environment's surface. Then the NSGA-II algorithm is used to find the improved solution during the generations evolution: each individual had about 20 seconds for its task, leading to 1,766 force points acquired. A total of 20 generations were used for this study, where each one had 20 individuals, resulting in a total of 400 experimental repetitions. The implementation was only possible due the use of the Robot Sensor Interface 2.3 library (Kuka 2009), implementing an impedance controller with a force-torque sensor from ATI Industrial Automation, model Delta SI-660-60 (ATI 2016).

The environment is part of a workbench used for general experimental purposes, being a fast-assembly aluminum square profile (Item24 2016), which had four other profiles fixed perpendicularly to it. Since the algorithm is supposed to enhance the impedance controller without knowing environment's properties, it is not necessary to calculate the equivalent stiffness of the workbench. The tool is a spindle holder used here due to its flat tip and nonlinear structure, due to the spindle hole.

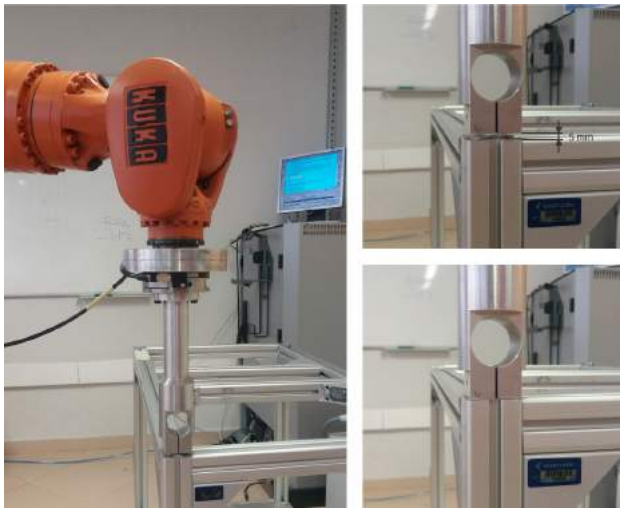

Figure 2: Experimental setup. Left - Kuka Robot KR16 with a 6 axis force/torque sensor attached to the wrist and the corresponding tool in contact with the aluminum frame; top right - initial position; bottom right - final position

The sketch of the implementation is illustrated at the block diagram of fig. 3. The arrows portray the information flow as inputs or outputs, and the blocks are the representation the abstraction in which device is located. The group *Robot and coupled dynamics* represents the real system composed by robot, sensor, tool, and environment, which returns the values of forces F_z to the computer algorithms. The computer, in its turn, is represented by the group *Algorithms and threads*, receives the force input data (F_z), calculate the objective metrics ($[T_r,\ TV,\ E_{ss}]^T$) via the *Data info* algorithm, and send these data as NSGA-II algorithm's input. Therefore, the GA will produce new gains for the *Impedance controller* ($[M,\ B,\ K]^T$), which operates at a constant 12 ms control loop time and is responsible to keep the robot working properly via *control actions* during the whole experiment.

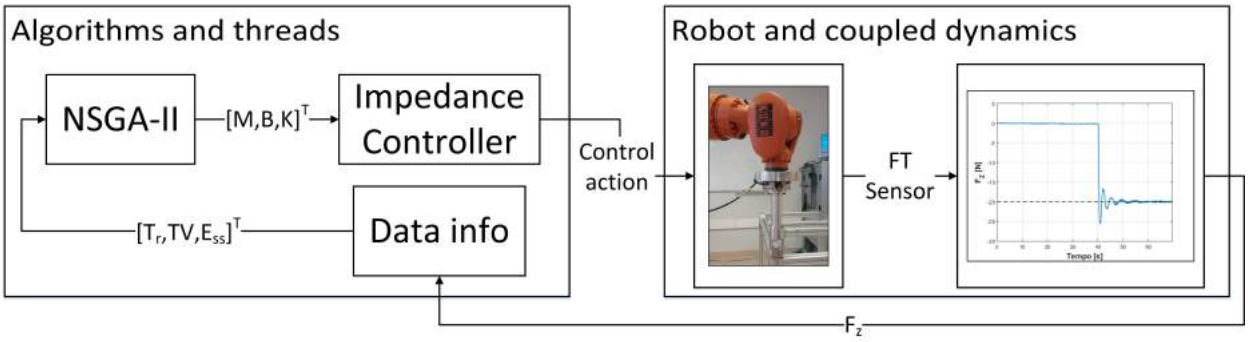

Figure 3: Information flow diagram. Left - running algorithms and real time threads for communication and GA functioning; right - real and environment setup with force acquisition

All codes run in C# within an i7 processor Windows 10 based PC. All communication is done using UDP/IP protocol network via XML data packages exchange between PC and robot controller. These packages contain information about robot position, force-torque values, and communication health (Kuka 2009). The thread *Impedance Controller* is respon-

sible to guarantee that the real time communication will not be lost, and it also calculates the impedance controller's control action, the one needed to move the robot and deal with the mechanical interaction.

At the moment the interaction controller is started, after all systems have been initialized, the robot's TCP is placed 5 mm distant from the environment. Since it will take some time to the tool establish contact, during this period the forces are basically zero, and this elapsed time is taken into account for the rise time metric. This way, one may notice that the values of T_r are higher in the order of a few seconds instead of milliseconds, which is usual for this metric.

The reference trajectory desired at eq. 1 is null, $x_0(t) = 0$. This simplifies the task of contact settling, where the desired force is $F_d(t) = 60\ N$ for all individuals. The whole experiment took around 2.5 hours to complete all individuals from all generations.

RESULTS

Experimental implementation led to satisfying results as the objective functions were properly diminished. This decrease is manifested in the series of graphics shown in figure 4 in which each color represents an individual. It can be noted that the rise time suffers a draw back through the generations and the amplitudes of oscillation, which is described by the total variation, are tightened. Also, the steady state error is decreased, since the last values, after 20 s, are closer to 60 N. It is possible to note the amount of time elapsed before the contact, which decreased from the 1st generation (starting almost at 10 s) to the 20th generation (less than 8 s).

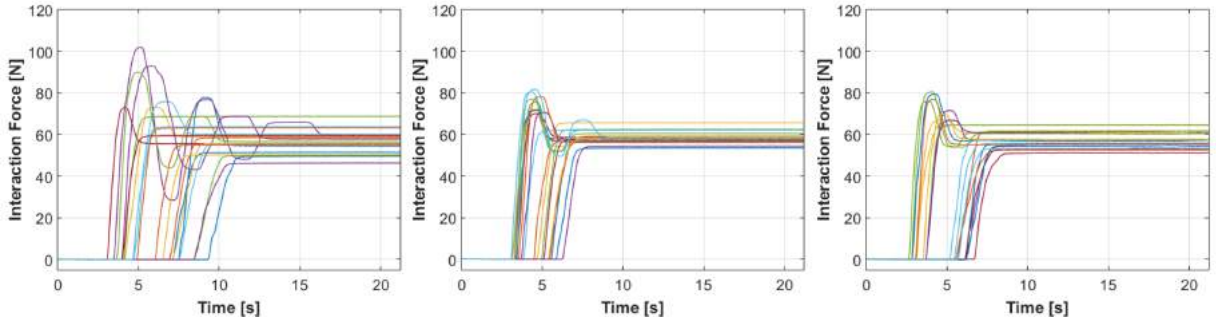

Figure 4: Interaction forces vector for each individual versus time: left, middle, and right the 1st, 10th, and 20th generations, respectively

Figure 5 illustrates the relationship between total variation, rise time and steady state error plot two by two. The set of graphics displayed by the first row of plots is the 1st generation of the metrics plot (5a), the second row is the 10th generation (5b), and third row, 20th generation (5c). Each dot represents an individual, i.e, an impedance controller with its respective time metric. The relationship between E_{ss} and T_r displays a small contraction over a 45-degree-diagonal direction looking at the first column of plots, since it was observed that steady state error and rise time decreased over the generations. A similar behavior may be noted for the second column of plots, between E_{ss} and TV, where the latter displayed a severe contraction. The most interesting Pareto front may be observed on the third column, where TV and T_r are shown: both decrease over time and a clear Pareto front may be seen. Although it is not intended yet to choose a specific controller, instead, to observe tendencies about the time metrics and the controllers, these Pareto fronts are helpful to pick a specific controller.

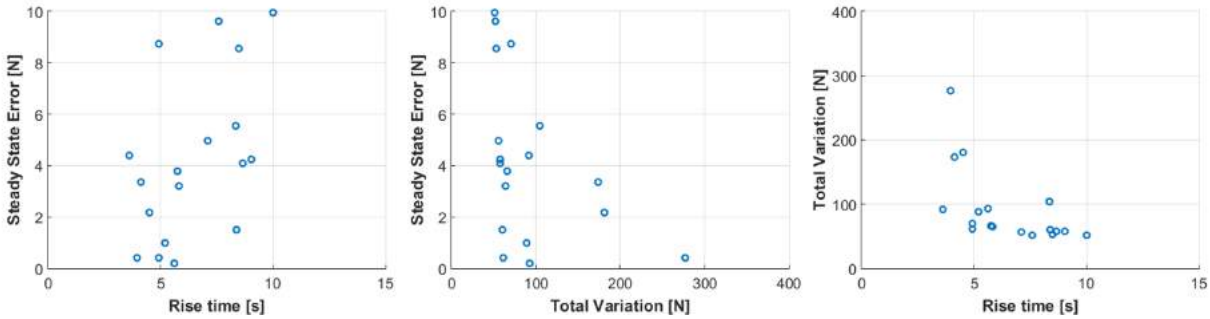

(a) 1st generation

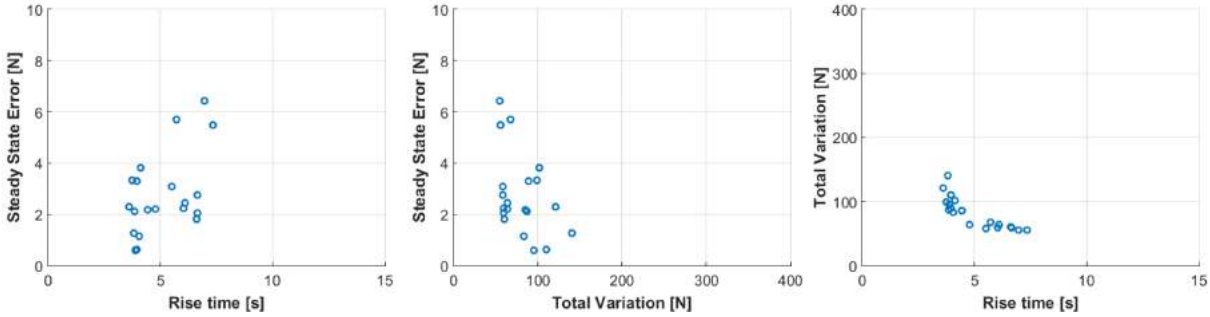

(b) 10th generation

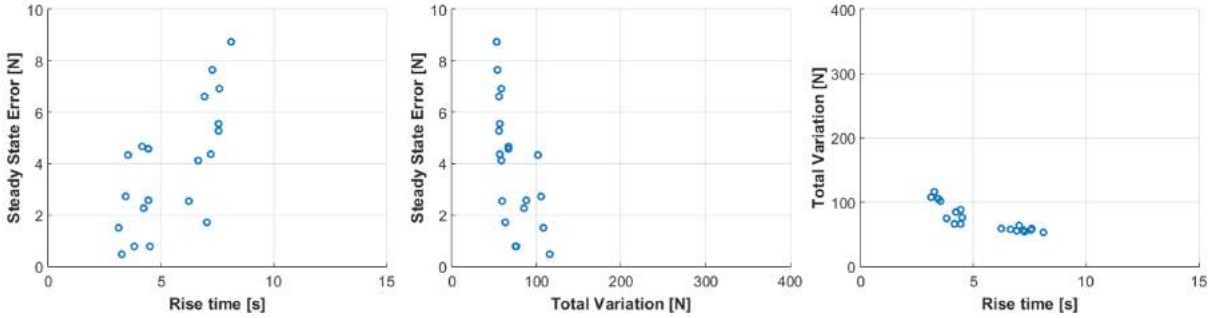

(c) 20th generation

Figure 5: Pareto fronts of E_{ss} x T_r (first column), E_{ss} x TV (second column), and TV x T_r (third column)

Figure 6 shows the relationship between the impedance controller damping, ζ, and the rise time of the coupled system dynamics. The colors represent the controller's gain B, which is red if $100\ Ns/m \leq B < 400\ Ns/m$, green if $400\ Ns/m \leq B < 700\ Ns/m$, and blue if $700\ Ns/m \leq B < 1000\ Ns/m$. Since (6a), (6b), and (6c) represent the 1st, 2nd, and 3rd generations, it is possible to notice that the values higher than $400\ Ns/m$ disappear after the 4th generation (6d). The values of B do not cross the border of $400\ Ns/m$ until the end of the experiment, represented by (6f). This is a counter intuitive result, since from the control theory point of view, assuming the robot as a second order system and the environment, first order, it would result in a second order system. Therefore, to obtain faster dynamics it should be expected to have smaller values of ζ. However, looking at fig. 6, smaller the damping, higher the rise time, what suggests that the real resulting system is not a second order, but higher. Also, the friction is not taken into account at any step in this work's model, although it is a major factor for contact modeling (Gilardi and Sharf 2002,Todorov 2010).

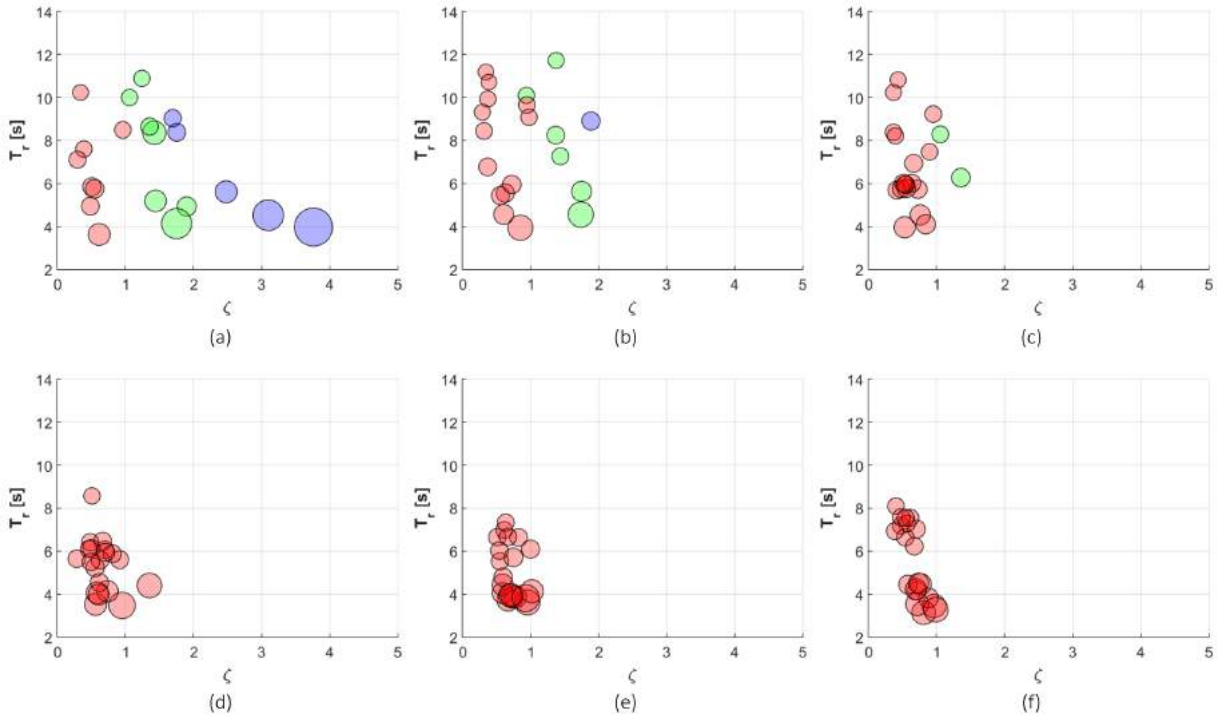

Figure 6: Plot of T_r x ζ for the (a) 1st, (b) 2nd, (c) 3rd, (d) 4th, (e) 10th, and (f) 20th generations

Another interesting observation that may be discussed is about the analysis of all individuals generated over the 20 generations of the optimization, where each blue dot is one impedance controller, however, all 400 individuals are in these plots (fig. 7). This approach is interesting because, while the data is resulting from an optimization process, each controller results in a respective time metric, for this particular set of environment+tool+robot.

Two tendencies are possible to note about the controller and the metrics T_r and TV. Plotting the latter values versus the stiffness (fig. 7 - middle), K, one may notice that lower the oscillations (small TV) are obtained via higher values of stiffness. In the other hand, looking for small values of T_r (fig. 7 - left), they require smaller values of the stiffness. The steady state error does not have a clear behavior, but it has a tendency to increase with the very high values of stiffness ($K > 3000\ N/m$).

From these two curves can be noted two trends: T_r leads to a linear fitting curve, which is denoted by the red dotted line (9); and TV is better described by an exponential fitting (10).

$$T_r(K) = 0.00264K + 0.7903 \tag{9}$$

$$TV(K) = 1376 * exp(-0.003006K) + 64.71 * exp(-6.424 * 10^{-5}K) \tag{10}$$

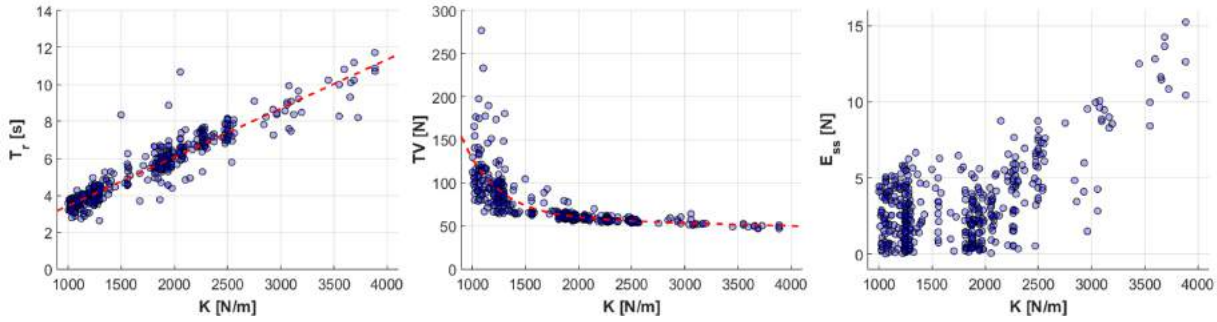

Figure 7: All individuals recorded over the optimization: T_r (left), TV (middle), E_{ss} (right) versus stiffness

The last analysis consists of the means and standard deviations for each controller parameter. Fig. 8 shows the tendency for each gain over the generations, where B and K show a convergence around 204.7 Ns/m and 1640.8 N/m respectively, between the 5th and 20th generations, respectively. M, however, does not display a clear convergence since it is more sensitive over small changes in its values.

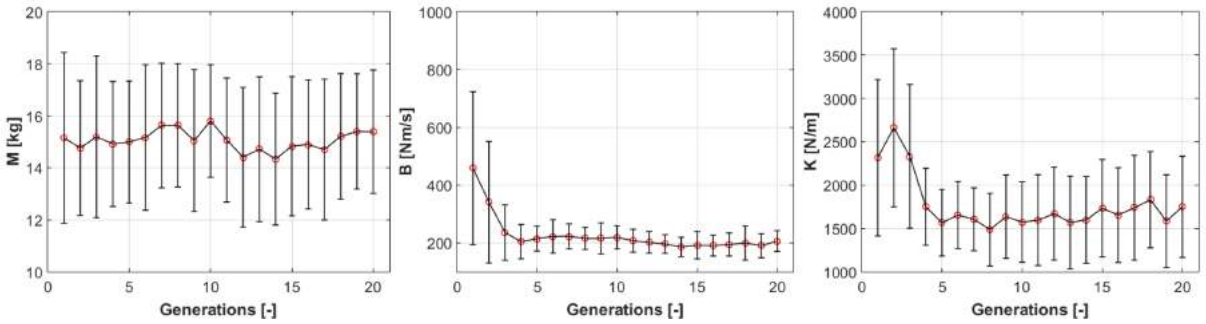

Figure 8: Controller parameters versus generations: M (left), B (middle), and K (right)

CONCLUSION

A hardware-in-the-loop optimization was implemented for better coupled dynamics between robot and environment. Results display that it is possible to implement this technique without worrying about non-modeled dynamics of nonlinearities, since the GA is capable to deal with them. Our method does not take into account environment characteristics, which makes an easier implementation. Also, although the fact that the whole experiment took around 2.5 hours to finish, 5th generation took approximately 40 minutes to complete, this means that the tendency for B and K were reach quickly.

An important consideration is about the B controller parameter: all individuals converge for the region below 400 Ns/m, what means a soft controller from the point of view of lumped systems. Only 4 generations were needed to higher values of B disappear. Moreover, higher values of ζ should lead to slower dynamics, instead, it is reaching a faster behavior. This indicates that the coupled system is not a second order, as the supposed earlier.

Relationships were possible to obtain between the values of stiffness and total variation with rise time. In addition, it was noticed a tendency of B and K to reach values below the half of possible limits.

Next steps of this work is to run the experiment for different environment, checking the robustness of the method. Also, the fitted curves are useful to enhance a theoretical model over a contact situation for this system setup, some studies may be disposed on this intention.

ACKNOWLEDGMENTS

We would like to acknowledge FAPESP (processes 2013/07276-1, 2015/07484-9 and 2015/24343-0), EMBRAER (cooperation project GSI-1168-15), CNPq and CAPES. Also, we would like to thank professor Maira M. Silva for her support over the development of this technique.

REFERENCES

ATI, 2016, "F/T Sensor: Delta". URL: http://www.ati-ia.com/products/ft/ft_models.aspx?id=Delta

Boyd, S. and Barratt, C., 1991, "Linear Controller Design: Limits of Performance", Prentice-Hall.

Buerger, S. P. and Hogan, N., 2007, Complementary Stability and Loop Shaping for Improved Human–Robot Interaction, "IEEE Transactions on Robotics 23(2)", 232–244.

Caurin, G. A. P., Siqueira, A. A. G., Andrade, K. O., Joaquim, R. C. and Krebs, H. I., 2011, "Adaptive strategy for multi-user robotic rehabilitation games.", Conference proceedings : ... Annual International Conference of the IEEE Engineering in Medicine and Biology Society. IEEE Engineering in Medicine and Biology Society. Annual Conference 2011, 1395–8.

Coutinho, F. and Cortesao, R., 2009, "Environment stiffness estimation with multiple observers", IECON Proceedings (Industrial Electronics Conference) pp. 1537–1542.

Coutinho, F. and Cortesao, R., 2012, "Comparison of position and force-based techniques for environment stiffness estimation in robotic tasks", IEEE International Conference on Intelligent Robots and Systems 1, 4933–4938.

Deb, K., Pratap, A., Agarwal, S. and Meyarivan, T., 2002, "A fast and elitist multiobjective genetic algorithm: NSGA-II", IEEE Transactions on Evolutionary Computation 6(2), 182–197.

Erickson, D., Weber, M. and Sharf, I., 2003, Contact Stiffness and Damping Estimation for Robotic Systems, "The International Journal of Robotics Research 22(1)", 41–57.

Fryman, J. and Matthias, B., 2012, Safety of industrial robots: From conventional to collaborative applications, in "7th German Conference on Robotics; Proceedings of ROBOTIK 2012", pp. 1–5.

Gilardi, G. and Sharf, I., 2002, "Literature survey of contact dynamics modelling", Mechanism and Machine Theory 37(10), 1213–1239.

Hogan, N., 1985, "Impedance control: An approach to manipulation: Parts I-III", Journal of Dynamic Systems, Measurement and Control, Transactions of the ASME 107(1), 1–7.

Hogan, N., 1987, Stable execution of contact tasks using impedance control, in "Proceedings. 1987 IEEE International Conference on Robotics and Automation", Vol. 4, Institute of Electrical and Electronics Engineers, pp. 1047–1054.

Item24, 2016, ”Construction Profile 8”. URL: http://www.item24us.com/products/product-catalog/products/construction-profiles-8.html

Jayender, J., Patel, R. and Nikumb, S., 2006, Robot-Assisted Catheter Insertion using Hybrid Impedance Control, in ”IEEE International Conference on Robotics and Automation, Florida, USA”.

Kuka, 2009, ”Kuka.RobotSensorInterface 2.3”.

Lahr, G. J. G., Soares, J. V. R., Garcia, H. B., Siqueira, A. A. G. and Caurin, G. A. P., 2016, Understanding the Implementation of Impedance Control in Industrial Robots, in ”LARS 2016 13rd Latin American Robotics Symposium”, Recife, Brasil.

Lange, F., Bertleff, W. and Suppa, M., 2013, Force and trajectory control of industrial robots in stiff contact, in ”2013 IEEE International Conference on Robotics and Automation”, IEEE, pp. 2927–2934.

Li, E., 2016, The robotic impedance controller multi-objective optimization design based on pareto optimality, in ”International Conference on Intelligent Computing”, Springer, pp. 413–423.

Love, L. and Book, W., 1995, ”Environmentestimationforenhancedimpedancecontrol”, Proc.IEEEInt.Conf.onRobotics and Automation (ICRA) 2(3), 1854–1859.

Mason, M. T., 1981, ”Compliance and Force Control for Computer Controlled Manipulators”, IEEE Transactions on Systems, Man, and Cybernetics 11(6), 418–432.

Mehdi, H. and Boubaker, O., 2011, ”Impedance controller tuned by particle swarm optimization for robotic arms”, International Journal of Advanced Robotic Systems 8(5), 93–103.

Ogata, K., 2010, Modern control engineering, Prentice-Hall.

Rao, S. S., 2009, Engineering Optimization, Vol. 56, John Wiley & Sons.

Salisbury, J., 1980, Active stiffness control of a manipulator in cartesian coordinates, in ”1980 19th IEEE Conference on Decision and Control including the Symposium on Adaptive Processes”, IEEE, pp. 95–100.

Siciliano, B. and Villani, L., 1999, Robot Force Control, Springer US, Boston, MA.

Todorov, E., 2010, Implicit nonlinear complementarity: A new approach to contact dynamics, in ”2010 IEEE International Conference on Robotics and Automation”, IEEE, pp. 2322–2329.

Villani, L. and de Schutter, J., 2008, Force Control, in B. Siciliano and O. Khatib, eds, ”Springer Handbook of Robotics”, Springer Berlin Heidelberg, Berlin, Heidelberg, Chapter 7:, pp. 161–184.

RESPONSIBILITY NOTICE

The author(s) is (are) the only responsible for the material included in this paper.